Nonlinear Dyn (2012) 69:705–720
DOI 10.1007/s11071-011-0298-6

ORIGINAL PAPER

Relaxed representations and improving stability in time-stepping analysis of three-dimensional structural nonlinear dynamics

Salvatore Lopez

Received: 27 June 2011 / Accepted: 6 December 2011 / Published online: 22 December 2011

Abstract In the present paper, we propose a representation of the discrete motion equations in structural nonlinear dynamics to obtain an improvement in the stability of time numerical integrations. A geometrically nonlinear total Lagrangian formulation for three-dimensional beam elements in the hypotheses of large rotations and small strains is presented. In this formulation, slopes are used instead of rotation parameters to compute the nonlinear representations of the strain measures in the inertial frame of reference. Such representations of the internal strains—rotations compatibility are then imposed in their time derivatives version. The results, related to Newmark approximations for the variations in the displacement and velocity vectors, show a significant increase in the range of stability of the time integration process and a reduction in the number of Newton iterations required in the time integration steps. The numerical tests, furthermore, show that the variation in the total energy in the time steps has bounded oscillations about the zero value.

Keywords Numerical stability · Time relaxed representation · Structural three-dimensional nonlinear dynamics

S. Lopez (✉)
Dipartimento di Modellistica per l'Ingegneria, Università della Calabria, 87030 Rende, Cosenza, Italy
e-mail: salvatore.lopez@unical.it

1 Introduction

Geometric nonlinearity in elastodynamics is an important field in structural analysis and in the last 30 years there has been extensive research into time integration algorithms. In particular, stability is an important issue because while unconditionally stable schemes can be recovered in linear dynamics, numerical instability frequently appears in nonlinear cases. In this context, to obtain stable solutions, schemes which demand the conservation or decrease in the total energy of the Hamiltonian system within each time step are extensively used.

Energy conserving algorithms in elastodynamics have already appeared in the works of Belytschko and Schoeberle [1] and Hughes et al. [2]. The energy-momentum method introduced by Simo and Tarnow [3, 4] preserves energy as well as linear and angular momentum in the time interval. Conservation properties are enforced in the equation of motion via Lagrange multipliers. Adaptive time stepping procedures (Kuhl and Ramm [5]) and controllable numerical dissipation (Hoff and Pahl [6], Chung and Hulbert [7]) can also be introduced to permit larger time steps and, consequently, to improve computational efficiency. Although finite difference methods appear to prevail in the literature on the numerical treatment of initial-value problems, a number of alternative finite element methods have been developed for the temporal discretization process. Weighted residual statement and the Galerkin finite element approach for the nu-

merical solution of the equations of motion has been employed in Zienkiewicz et al. [8] and in Lasaint and Raviart [9]. More recently, time finite elements, where the Newmark family formulas can be recovered by the choice of representative constants and the algorithmic energy conservation is implicitly preserved have been carried out (see Betsch and Steinmann [10] and related bibliography).

In this paper, we present an extension of the approach described in [11] for time-stepping nonlinear analysis to the three-dimensional case. In [11], the introduction of strains as additional local variables to the representation of the internal energy leads to a significant increase in the range of stability of the classical Newmark method. In particular, the related additional equations are governed by a dynamical representation of the internal strains—rotations compatibility. In such a dynamical representation, then the expressions that define strain measures are imposed in their time derivatives version. Here, the three-dimensional nonlinear models are established by the use of Lagrangian multipliers. Related constraint equations represent the nonlinear definition of the internal strains as a function of the rotational descriptors. Thus, the imposition of such equations is the strong form of the strain definitions while the time derivative of constraint equations represents the related relaxed form.

Of course, the use of the strong internal constraint equations can be replaced by the intrinsic definition of the related parameters by obtaining, however, similar computational characteristics in terms of number of time-steps and approximation properties. The use of the time relaxed description of the compatibility conditions between deformation and rotational parameters, instead, leads to an appreciable increase in the range of stability of the time integration scheme. The increase in computational effort due to the introduction of new unknowns and the loss of symmetry in the iteration matrix is therefore balanced by the reduction in the number of Newton iterations required in the time integration steps.

Note that the described approach, although quite different, has analogies with the procedure of index reduction of the differential-algebraic equations (DAEs); see, e.g., Gear and Petzold [12], Bachmann et al. [13] and Mattsson and Söderlind [14]. Such a procedure is based on a reduction of the DAE problem to an ordinary differential equation (ODE) by a number of differentiations of the given constraint equations. Differentiations are carried out until the elimination of the related Lagrange multipliers typically in terms of velocities and accelerations is possible. The resulting ODE can then be integrated using effective explicit algorithms, mainly with regard to the stability. In the presented approach, one time differentiation of the constraint equations is performed. Furthermore, such relaxed constraints are used to define the Lagrangian extended functional and not directly employed as motion equations. Thus, Lagrange multipliers and their derivatives are also present in the motion equations. These quantities are coupled with the kinematical unknowns and are involved in an implicit integration process. Finally, constraints are not intrinsic equations of the mechanical model here but are definitions of mechanical parameters which can already be eliminated directly.

As regards beam element modeling, the corotational approach is one of the classical ways for modeling three-dimensional elastic frame structures for small strains with large displacements. The motion of the continuous medium is decomposed into a rigid body motion followed by a pure deformation. Then the nonlinear motion is obtained by joining the linear kinematic with a rigid body motion that is recovered by the use of orthogonal transformation matrices. The evolution of the corotational approach can be traced by referring to the works: Belytschko and Hsieh [15], Argyris [16], Rankin and Nour-Omid [17], Cardona and Geradin [18], Crisfield [19] and Ibrahimbegović et al. [20]. These techniques, however, have to be supported by a robust and economical definition of the rotated local reference system. Basically, attention has to be paid to avoid singularities in the transformation matrices for several angles and complex manipulations to overcome nonconservative descriptions due to the noncommutativity of rotations.

Here, we use a small strains—finite rotations formulation of a three-dimensional finite element beam without the use of rotation parameterizations, while preserving the robustness and simplicity of the analysis (see [21]). Based on the Timoshenko beam theory, the actual configuration of the element is rigidly translated and rotated, and deformed according to the selected linear modes. Rigid and deformation modes are referred to the nodes of the element by a Total Lagrangian formulation. The nonlinear rigid motion is recovered by referring to three unit and mutually orthogonal vectors attached to the nodes of the beam

element. All nine components of such vectors in the global inertial frame of reference are assumed as unknown. As demonstrated in [22], the rotational degree-of-freedom of the element is reduced to only three by six well-posed constraint conditions.

An approach where the nine components of the rotation matrix are used directly has already been presented by Betsch and Steinmann [23, 24] in the finite rotations analysis of rigid bodies and beams. Orthonormality of the directors is enforced by using six scalar products. In particular, three unit length and three orthogonality conditions are imposed on the directors by using the scalar products among them and reciprocally, respectively. Here, instead three scalar products and one cross product are used to define the constraint conditions. In detail, two unit length and one orthogonality conditions are imposed by scalar products while the complete definition of a director is obtained by referring to a cross product. In this way, we demonstrate that the present formulation proves to be well posed for any finite rotations. Furthermore, a reduction in the number of unknowns is possible here using the cross product between two directors as an explicit definition of the components of third director.

The remainder of the paper is organized as follows. In Sect. 2, the adopted description of the finite rotations in elastic frame structures is given. In Sect. 3, we define the kinematics of the beam element while related energetic quantities are evaluated in Sect. 4. As particular cases of the given beam element description, the motion equations of prismatic bodies and mass particles are deduced in Sect. 5. Section 6 contains the semidiscrete motion equations and related time-integration algorithm. Examples of applications of the proposed scheme are given in Sect. 7. Final conclusions are drawn in Sect. 8.

2 Description of the finite rotations

In the corotational approach, the motion of the body is decomposed into a rigid motion followed by a pure deformation performed in a local corotational frame that rotates and translates with each element. So, all the nonlinearity of the problem derives essentially from the change of reference from the global fixed frame to the local one, the strain energy being governed by their relative rotations. In this way, the main difficulty is the presence of finite rotations in finite kinematics that noticeably complicates the algebra for obtaining kinematic expressions. In particular, finite 3D rotations must be described through rotation matrices which lie in a nonlinear manifold.

In the corotational analysis carried out here, we refer to three unit and mutually orthogonal unknown vectors $\mathbf{E}^{\xi}$, $\mathbf{E}^{\eta}$, and $\mathbf{E}^{\zeta}$ attached to the body and defined in the global inertial frame of reference (x, y, z). Classically, these unknown vectors, defining rigid rotation in the current configuration, are obtained by rotating the corresponding known vectors $\mathbf{e}^{\xi}$, $\mathbf{e}^{\eta}$, and $\mathbf{e}^{\zeta}$ of the initial configuration. This mapping is realized by an $\mathbf{R}$ rotation matrix. The Rodrigues formula, then allows $\mathbf{R}$ to be expressed in terms of the quantities lying in a vector space and reduces to a three independent parameter representation:

$$\begin{aligned}\mathbf{R}(\boldsymbol{\phi}) &= \exp\big(\mathbf{S}(\boldsymbol{\phi})\big) \\ &= I + \mathbf{S}(\boldsymbol{\phi}) + \frac{1}{2}\mathbf{S}(\boldsymbol{\phi})^2 + \cdots = \sum_{n}^{\infty} \frac{1}{n!}\mathbf{S}(\boldsymbol{\phi})^n, \quad (1)\end{aligned}$$

which uses the rotation vector $\boldsymbol{\phi} = \{\phi_\xi, \phi_\eta, \phi_\zeta\}$ and the skew-symmetric matrix

$$\mathbf{S}(\boldsymbol{\phi}) = \begin{bmatrix} 0 & -\phi_\zeta & \phi_\eta \\ \phi_\zeta & 0 & -\phi_\xi \\ -\phi_\eta & \phi_\xi & 0 \end{bmatrix}. \quad (2)$$

Here, all nine components of $\mathbf{E}^{\xi}$, $\mathbf{E}^{\eta}$, and $\mathbf{E}^{\zeta}$ vectors are assumed as unknown. As demonstrated in [22], by the following six well-posed constraint conditions:

$$\begin{aligned} g_E^{\eta} &= \mathbf{E}^{\eta} \cdot \mathbf{E}^{\eta} - 1 = 0, \\ g_E^{\zeta} &= \mathbf{E}^{\zeta} \cdot \mathbf{E}^{\zeta} - 1 = 0, \\ g_E^{\eta\zeta} &= \mathbf{E}^{\eta} \cdot \mathbf{E}^{\zeta} = 0, \\ \mathbf{g}_E^{\xi} &= \mathbf{E}^{\eta} \times \mathbf{E}^{\zeta} - \mathbf{E}^{\xi} = \mathbf{0}, \end{aligned} \quad (3)$$

the rotational degrees of freedom are reduced just to three. Of course, six conditions being imposed, the degrees of freedom are at least three. To show also that the degrees of freedom are at most three, it was demonstrated that nullity($\mathbf{G}$) is at most three in the solution point, where $\mathbf{G}$ is the Jacobian matrix related to the (3) $\mathbf{g}_E = \mathbf{0}$ system.

It should be emphasized that the number of arithmetical operations between the two approaches are comparable if we stop the exponential map expansion at a very low order. In this case, however, a poor accuracy of the co-rotational approach results, especially

for appreciably large rotations. On the contrary, in total Lagrange descriptions, the proposed approach is insensitive to the rotation values and still effective from a computational point of view.

3 Kinematics of the beam element

We refer to the referential coordinate ξ along the element beam centerline $-h_\xi/2 \le \xi \le +h_\xi/2$. In the following, we denote with i, j and o the nodes respectively in $\xi = -h_\xi/2$, $\xi = +h_\xi/2$ and $\xi = 0$. Along the beam centerline, we define the displacement vector $\mathbf{u}(\xi) = \{u(\xi), v(\xi), w(\xi)\}$ and three mutually orthogonal vectors $\mathbf{E}^\xi(\xi) = \{E_x^\xi(\xi), E_y^\xi(\xi), E_z^\xi(\xi)\}$, $\mathbf{E}^\eta(\xi) = \{E_x^\eta(\xi), E_y^\eta(\xi), E_z^\eta(\xi)\}$, $\mathbf{E}^\zeta(\xi) = \{E_x^\zeta(\xi), E_y^\zeta(\xi), E_z^\zeta(\xi)\}$, in the global inertial frame of reference (x, y, z). Director vectors $\mathbf{E}^\eta$ and $\mathbf{E}^\zeta$ are along the principal axes of inertia of the cross-section. Let $\mathbf{E}^\xi$, $\mathbf{E}^\eta$ and $\mathbf{E}^\zeta$ vectors be the columns of the matrix $\mathbf{E}(\xi)$:

$$\mathbf{E}(\xi) = \left[\mathbf{E}^\xi(\xi) \,\middle|\, \mathbf{E}^\eta(\xi) \,\middle|\, \mathbf{E}^\zeta(\xi)\right]. \tag{4}$$

The $\mathbf{E}(\xi)$ orthonormal matrix is obtained by using director vectors at the i, j, and o nodes and constrained to the (3) conditions. In particular, we will use unknown $\mathbf{E}_o = \mathbf{E}(0)$ to represent the large three-dimensional rotations of the local frame of reference of the beam element. As mentioned, the initial unit vector in the ξ, η, and ζ element direction, finally, will be denoted by $\mathbf{e}^\xi$, $\mathbf{e}^\eta$, and $\mathbf{e}^\zeta$, respectively (see Fig. 1).

In the beam element, global displacement vector $\mathbf{u}(\xi)$ is composed of rigid and deformation components. In particular, we refer to the $\bar{\mathbf{u}} = (\bar{u}(\xi), \bar{v}(\xi), \bar{w}(\xi))$ rigid displacements defined in the initial frame of reference while the deformation $\tilde{\mathbf{u}}(\xi) = (\tilde{u}(\xi), \tilde{v}(\xi), \tilde{w}(\xi))$ displacements and $\tilde{\boldsymbol{\theta}} = (\tilde{\theta}^\xi(\xi), \tilde{\theta}^\eta(\xi), \tilde{\theta}^\zeta(\xi))$ rotations are defined in the local rigidly rotated frame of reference. The deformation kinematics is assumed by the linear interpolations

$$\tilde{u} = \varepsilon_o \xi, \qquad \tilde{v} = \varphi_o^\eta \xi, \qquad \tilde{w} = \varphi_o^\zeta \xi, \tag{5}$$

for displacements and the quadratic interpolations

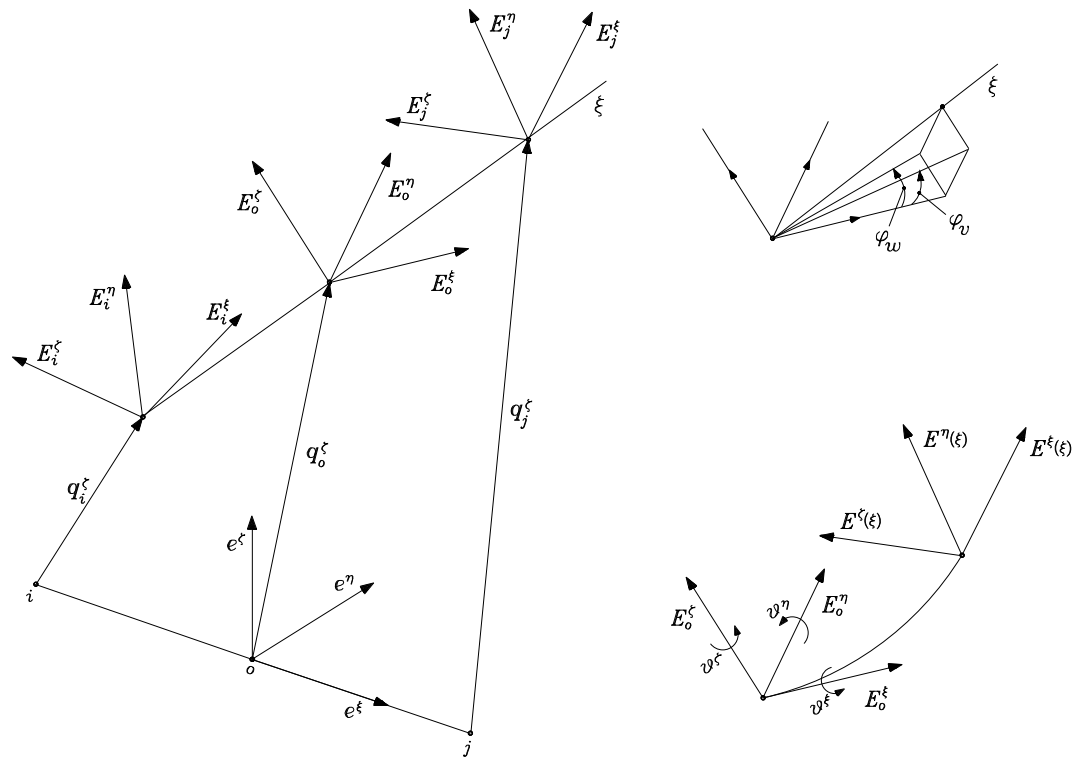

Fig. 1 Total Lagrangian co-rotational formulation: element kinematics and coordinate systems

$$\tilde{\theta}^{\eta} = \frac{\theta_j^{\eta} - \theta_i^{\eta}}{h_{\xi}}\xi + 2\frac{\theta_i^{\eta} + \theta_j^{\eta}}{h_{\xi}^2}\xi^2,$$
$$\tilde{\theta}^{\zeta} = \frac{\theta_j^{\zeta} - \theta_i^{\zeta}}{h_{\xi}}\xi + 2\frac{\theta_i^{\zeta} + \theta_j^{\zeta}}{h_{\xi}^2}\xi^2, \tag{6}$$

for flexural rotations. The kinematics of the element is then completed by defining the local $\tilde{\theta}^{\xi}$ torque rotation about the beam centerline. As in (6), we assume

$$\tilde{\theta}^{\xi} = \frac{\theta_j^{\xi} - \theta_i^{\xi}}{h_{\xi}}\xi + 2\frac{\theta_i^{\xi} + \theta_j^{\xi}}{h_{\xi}^2}\xi^2. \tag{7}$$

Note that zero local rotations at the center of the element are assumed. Rigid kinematics, then, will be represented by the nodal displacement components and the degrees of freedom of the vectors $\mathbf{E}_o^{\xi}$ attached to the central node.

Based on the above definitions, local rotations and director components are now linked by the field vector operations

$$\mathbf{E}^{\xi}(\xi) = \mathbf{E}_o^{\xi} + \tilde{\theta}^{\eta}(\xi)\mathbf{E}_o^{\eta} + \tilde{\theta}^{\zeta}(\xi)\mathbf{E}_o^{\zeta},$$
$$\mathbf{E}^{\eta}(\xi) = -\tilde{\theta}^{\eta}(\xi)\mathbf{E}_o^{\xi} + \mathbf{E}_o^{\eta} + \tilde{\theta}^{\xi}(\xi)\mathbf{E}_o^{\zeta}, \tag{8}$$
$$\mathbf{E}^{\zeta}(\xi) = -\tilde{\theta}^{\zeta}(\xi)\mathbf{E}_o^{\xi} - \tilde{\theta}^{\xi}(\xi)\mathbf{E}_o^{\eta} + \mathbf{E}_o^{\zeta}.$$

As proven, vectors $\mathbf{E}_o^{\xi}$, $\mathbf{E}_o^{\eta}$, and $\mathbf{E}_o^{\zeta}$ are unit and mutually orthogonal at the solution points. Then, at the first order, $\mathbf{E}^{\xi}(\xi)$, $\mathbf{E}^{\eta}(\xi)$, and $\mathbf{E}^{\zeta}(\xi)$, there are also three unit and mutually orthogonal vectors and they completely define the global orientation of the cross-section. We note that the first order accuracy of the (8) representations leads to local evaluations consistent with the small strains hypotheses.

By evaluating (8) relations for $\xi = -h_{\xi}/2$ and $\xi = h_{\xi}/2$, respectively, in the i and j nodes, and by using orthonormality of the directors, we can write

$$\theta_j^{\xi} - \theta_i^{\xi} = \frac{1}{2}\left(\mathbf{E}_i^{\zeta}\cdot\mathbf{E}_j^{\eta} - \mathbf{E}_i^{\eta}\cdot\mathbf{E}_j^{\zeta}\right),$$
$$\theta_j^{\eta} - \theta_i^{\eta} = \frac{1}{2}\left(\mathbf{E}_i^{\eta}\cdot\mathbf{E}_j^{\xi} - \mathbf{E}_i^{\xi}\cdot\mathbf{E}_j^{\eta}\right), \tag{9}$$
$$\theta_j^{\zeta} - \theta_i^{\zeta} = \frac{1}{2}\left(\mathbf{E}_i^{\zeta}\cdot\mathbf{E}_j^{\xi} - \mathbf{E}_i^{\xi}\cdot\mathbf{E}_j^{\zeta}\right),$$

and

$$\theta_j^{\xi} + \theta_i^{\xi} = \frac{1}{2}\left[\mathbf{E}_o^{\zeta}\cdot\left(\mathbf{E}_i^{\eta} + \mathbf{E}_j^{\eta}\right) - \mathbf{E}_o^{\eta}\cdot\left(\mathbf{E}_i^{\zeta} + \mathbf{E}_j^{\zeta}\right)\right],$$
$$\theta_j^{\eta} + \theta_i^{\eta} = \frac{1}{2}\left[\mathbf{E}_o^{\eta}\cdot\left(\mathbf{E}_i^{\xi} + \mathbf{E}_j^{\xi}\right) - \mathbf{E}_o^{\xi}\cdot\left(\mathbf{E}_i^{\eta} + \mathbf{E}_j^{\eta}\right)\right], \tag{10}$$
$$\theta_j^{\zeta} + \theta_i^{\zeta} = \frac{1}{2}\left[\mathbf{E}_o^{\zeta}\cdot\left(\mathbf{E}_i^{\xi} + \mathbf{E}_j^{\xi}\right) - \mathbf{E}_o^{\xi}\cdot\left(\mathbf{E}_i^{\zeta} + \mathbf{E}_j^{\zeta}\right)\right].$$

Furthermore, by referring to the centerline points, we now define rigid and deformation components in the initial frame of reference by

$$\bar{u}(\xi) = u_o + \xi E_{ox}^{\xi} - \xi,$$
$$\bar{v} = v_o + \xi E_{ox}^{\eta}, \tag{11}$$
$$\bar{w} = w_o + \xi E_{ox}^{\zeta},$$

and

$$\hat{u}(\xi) = \varepsilon_o\xi E_{ox}^{\xi} + \varphi_o^{\eta}\xi E_{ox}^{\eta} + \varphi_o^{\zeta}\xi E_{ox}^{\zeta},$$
$$\hat{v}(\xi) = \varepsilon_o\xi E_{oy}^{\xi} + \varphi_o^{\eta}\xi E_{oy}^{\eta} + \varphi_o^{\zeta}\xi E_{oy}^{\zeta}, \tag{12}$$
$$\hat{w}(\xi) = \varepsilon_o\xi E_{oz}^{\xi} + \varphi_o^{\eta}\xi E_{oz}^{\eta} + \varphi_o^{\zeta}\xi E_{oz}^{\zeta},$$

respectively. Then, in the vectorial notation, the motion of the ξ point is described as

$$\mathbf{u} = \mathbf{u}_o + \xi\mathbf{E}_o^{\xi} - \xi\mathbf{e}^{\xi} + \varepsilon_o\xi\mathbf{E}_o^{\xi} + \varphi_o^{\eta}\xi\mathbf{E}_o^{\eta} + \varphi_o^{\zeta}\xi\mathbf{E}_o^{\zeta}. \tag{13}$$

Also here, by evaluating (13) relations for nodal coordinates $\xi = -h_{\xi}/2$, $\xi = h_{\xi}/2$, and by using orthonormality of the directors, we deduce that

$$\mathbf{u}_o = \frac{1}{2}(\mathbf{u}_i + \mathbf{u}_j) \tag{14}$$

is the central point displacement and

$$g_I^{\xi} = \varepsilon_o - \frac{1}{h_{\xi}}\left[\mathbf{E}_o^{\xi}\cdot(\mathbf{u}_j - \mathbf{u}_i) - h_{\xi} + h_{\xi}E_{ox}^{\xi}\right] = 0,$$
$$g_I^{\eta} = \varphi_o^{\eta} - \frac{1}{h_{\xi}}\left[\mathbf{E}_o^{\eta}\cdot(\mathbf{u}_j - \mathbf{u}_i) + h_{\xi}E_{ox}^{\eta}\right] = 0, \tag{15}$$
$$g_I^{\zeta} = \varphi_o^{\zeta} - \frac{1}{h_{\xi}}\left[\mathbf{E}_o^{\zeta}\cdot(\mathbf{u}_j - \mathbf{u}_i) + h_{\xi}E_{ox}^{\zeta}\right] = 0,$$

are the expressions of the axial and shear deformations as a function of nodal displacement and director components. In the following, the defined g_I^{ξ}, g_I^{η}, and g_I^{ζ} expressions of internal strain evaluations will be used in the description of the improving solution scheme.

As can be seen, unknown nodal components completely define the (5)–(7) linearized deformation kinematics of the beam element by (9)–(10) and (15) expressions. Nonlinear rigid kinematics, instead, is described by the displacement vector in (14) and the unknown director vectors $\mathbf{E}_o$ at the central node. The remaining unknown components of the element are the displacements $\mathbf{u}_i$, $\mathbf{u}_j$ and the director vectors $\mathbf{E}_i$, $\mathbf{E}_j$ at the boundary nodes.

4 Evaluation of energetic quantities of the beam element

We consider the referential coordinates (ξ, η, ζ) in the element, where η and ζ are the thickness coordinates in the $\mathbf{e}^\eta$ and $\mathbf{e}^\zeta$ directions, respectively. By denoting with $\mathbf{u}_P(\xi,\eta,\zeta) = \{u_P(\xi,\eta,\zeta), v_P(\xi,\eta,\zeta), w_P(\xi,\eta,\zeta)\}$ the displacement of the generic point P in the element represented in the global reference frame, we can refer respectively to the expression

$$\bar{\mathbf{u}}_P = \mathbf{u}_o + \xi\left(\mathbf{E}_o^\xi - \mathbf{e}^\xi\right) + \eta\left(\mathbf{E}_o^\eta - \mathbf{e}^\eta\right) + \zeta\left(\mathbf{E}_o^\zeta - \mathbf{e}^\zeta\right) \tag{16}$$

for the rigid and to expression

$$\begin{aligned}\hat{\mathbf{u}}_P = {} & \tilde{u}\mathbf{E}_o^\xi + \tilde{v}\mathbf{E}_o^\eta + \tilde{w}\mathbf{E}_o^\zeta - \left(\tilde{\theta}^\zeta\eta + \tilde{\theta}^\eta\zeta\right)\mathbf{E}_o^\xi \\ & + \tilde{\theta}^\xi\left(\eta\mathbf{E}_o^\zeta - \zeta\mathbf{E}_o^\eta\right)\end{aligned} \tag{17}$$

for the deformation components of the motion $\mathbf{u}_P = \bar{\mathbf{u}}_P + \hat{\mathbf{u}}_P$.

The principal energetic quantities involved are the kinetic, potential, and external energy:

$$\begin{aligned} T &= \frac{1}{2}\int_V \rho\dot{\mathbf{u}}_P\cdot\dot{\mathbf{u}}_P\,dV, \\ U &= \frac{1}{2}\int_V \boldsymbol{\varepsilon}_P : \boldsymbol{\sigma}_P\,dV, \\ W &= \int_V \mathbf{p}\cdot\mathbf{u}_P\,dV, \end{aligned} \tag{18}$$

respectively. In (18), the dot denotes derivatives with respect to time t, V the volume of beam, $\mathbf{p}$ the vector of external loads and ρ the mass density. Furthermore, $\boldsymbol{\varepsilon}_P$ and $\boldsymbol{\sigma}_P$ are the infinitesimal strain and stress tensors in the body, respectively.

Kinetic energy is now evaluated by referring to the following expression of the velocity vector:

$$\begin{aligned}\dot{\mathbf{u}}_P = {} & \dot{\mathbf{u}}_o + \xi\dot{\mathbf{E}}_o^\xi + \eta\dot{\mathbf{E}}_o^\eta + \zeta\dot{\mathbf{E}}_o^\zeta + \dot{\tilde{u}}\mathbf{E}_o^\xi + \dot{\tilde{v}}\mathbf{E}_o^\eta + \dot{\tilde{w}}\mathbf{E}_o^\zeta \\ & - \left(\dot{\tilde{\theta}}^\zeta\eta + \dot{\tilde{\theta}}^\eta\zeta\right)\mathbf{E}_o^\xi + \dot{\tilde{\theta}}^\xi\left(\eta\mathbf{E}_o^\zeta - \zeta\mathbf{E}_o^\eta\right),\end{aligned} \tag{19}$$

obtained by time differentiation of $\mathbf{u}_P$ and by truncation of the deformation measures to the zero order. The integration over the section area A of the square of the velocity in (19) leads to:

$$\begin{aligned}&\int_A \dot{\mathbf{u}}_P\cdot\dot{\mathbf{u}}_P dA \\ &\quad = A\dot{\mathbf{u}}_o\cdot\dot{\mathbf{u}}_o + \xi^2 A\dot{\mathbf{E}}_o^\xi\cdot\dot{\mathbf{E}}_o^\xi + J_\zeta\dot{\mathbf{E}}_o^\eta\cdot\dot{\mathbf{E}}_o^\eta \\ &\qquad + J_\eta\dot{\mathbf{E}}_o^\zeta\cdot\dot{\mathbf{E}}_o^\zeta + 2\xi A\dot{\mathbf{u}}_o\cdot\dot{\mathbf{E}}_o^\xi \\ &\qquad + A\dot{\tilde{\mathbf{u}}}\cdot\dot{\tilde{\mathbf{u}}} + J_o\dot{\tilde{\theta}}^{\xi^2} + J_\eta\dot{\tilde{\theta}}^{\eta^2} + J_\zeta\dot{\tilde{\theta}}^{\zeta^2} \\ &\qquad + 2A\left(\dot{\tilde{u}}\mathbf{E}_o^\xi + \dot{\tilde{v}}\mathbf{E}_o^\eta + \dot{\tilde{w}}\mathbf{E}_o^\zeta\right)\cdot\left(\dot{\mathbf{u}}_o + \xi\dot{\mathbf{E}}_o^\xi\right) \\ &\qquad + 2\dot{\tilde{\theta}}^\xi\left(J_\zeta\dot{\mathbf{E}}_o^\eta\cdot\mathbf{E}_o^\zeta - J_\eta\dot{\mathbf{E}}_o^\zeta\cdot\mathbf{E}_o^\eta\right) \\ &\qquad - 2\left(J_\eta\dot{\tilde{\theta}}^\eta\dot{\mathbf{E}}_o^\zeta + J_\zeta\dot{\tilde{\theta}}^\zeta\dot{\mathbf{E}}_o^\eta\right)\cdot\mathbf{E}_o^\xi,\end{aligned} \tag{20}$$

where J_η and J_ζ are the second moments of area about the related principal axes while J_o is the polar moment. By defining the vector $\boldsymbol{\gamma} = (\varepsilon_o, \varphi_o^\eta, \varphi_o^\zeta)$, kinetic energy is now computed by further integration over the beam centerline:

$$\begin{aligned}&\frac{1}{2}\int_{-h_\xi/2}^{h_\xi/2}\int_A \rho\dot{\mathbf{u}}_P\cdot\dot{\mathbf{u}}_P\,dA\,d\xi \\ &\quad = \frac{1}{2}\rho\Big\{h_\xi A\dot{\mathbf{u}}_o\cdot\dot{\mathbf{u}}_o + AJ_\xi\dot{\mathbf{E}}_o^\xi\cdot\dot{\mathbf{E}}_o^\xi \\ &\qquad + h_\xi J_\zeta\dot{\mathbf{E}}_o^\eta\cdot\dot{\mathbf{E}}_o^\eta + h_\xi J_\eta\dot{\mathbf{E}}_o^\zeta\cdot\dot{\mathbf{E}}_o^\zeta \\ &\qquad + AJ_\xi\dot{\boldsymbol{\gamma}}\cdot\dot{\boldsymbol{\gamma}} + 2AJ_\xi\mathbf{E}_o^\xi\cdot\mathbf{E}_o\cdot\dot{\boldsymbol{\gamma}} \\ &\qquad + \frac{h_\xi}{12}\left(J_o\dot{D}\theta^{\xi^2} + J_\eta\dot{D}\theta^{\eta^2} + J_\zeta\dot{D}\theta^{\zeta^2}\right) \\ &\qquad + \frac{h_\xi}{20}\left(J_o\dot{S}\theta^{\xi^2} + J_\eta\dot{S}\theta^{\eta^2} + J_\zeta\dot{S}\theta^{\zeta^2}\right) \\ &\qquad + \frac{h_\xi}{3}\Big[\dot{S}\theta^\xi\left(J_\zeta\dot{\mathbf{E}}_o^\eta\cdot\mathbf{E}_o^\zeta - J_\eta\dot{\mathbf{E}}_o^\zeta\cdot\mathbf{E}_o^\eta\right) \\ &\qquad - \left(J_\eta\dot{S}\theta^\eta\dot{\mathbf{E}}_o^\zeta + J_\zeta\dot{S}\theta^\zeta\dot{\mathbf{E}}_o^\eta\right)\cdot\mathbf{E}_o^\xi\Big]\Big\},\end{aligned} \tag{21}$$

with the positions $J_\xi = h_\xi^3/12$, $\boldsymbol{D\theta} = (\theta_j^\xi - \theta_i^\xi, \theta_j^\eta - \theta_i^\eta, \theta_j^\zeta - \theta_i^\zeta)$ and $\boldsymbol{S\theta} = (\theta_i^\xi + \theta_j^\xi, \theta_i^\eta + \theta_j^\eta, \theta_i^\zeta + \theta_j^\zeta)$.

Finally, by introducing the geometrical coefficient matrices $\mathbf{J}_A = \mathrm{diag}(J_o, J_\eta, J_\zeta)$ and $\mathbf{J}_V = \mathrm{diag}(AJ_\xi, h_\xi J_\eta, h_\xi J_\zeta)$ we can write:

$$\begin{aligned}T = {} & \frac{1}{2}\rho\Big\{V\dot{\mathbf{u}}_o\cdot\dot{\mathbf{u}}_o + \dot{\mathbf{E}}_o\cdot\mathbf{J}_V\cdot\dot{\mathbf{E}}_o \\ & + AJ_\xi\left(\dot{\boldsymbol{\gamma}} + 2\dot{\mathbf{E}}_o^\xi\cdot\dot{\mathbf{E}}_o\right)\cdot\dot{\boldsymbol{\gamma}} \\ & + \frac{h_\xi}{12}\dot{\boldsymbol{D\theta}}\cdot\mathbf{J}_A\cdot\dot{\boldsymbol{D\theta}} + \frac{h_\xi}{20}\dot{\boldsymbol{S\theta}}\cdot\mathbf{J}_A\cdot\dot{\boldsymbol{S\theta}} \\ & + \frac{h_\xi}{3}\Big[\dot{S}\theta^\xi\left(J_\zeta\dot{\mathbf{E}}_o^\eta\cdot\mathbf{E}_o^\zeta - J_\eta\dot{\mathbf{E}}_o^\zeta\cdot\mathbf{E}_o^\eta\right) \\ & - \left(J_\eta\dot{S}\theta^\eta\dot{\mathbf{E}}_o^\zeta + J_\zeta\dot{S}\theta^\zeta\dot{\mathbf{E}}_o^\eta\right)\cdot\mathbf{E}_o^\xi\Big]\Big\}.\end{aligned} \tag{22}$$

In (22), the rigid, deformation and mixed kinetic terms can be recognized. In particular, note how the term $\dot{\mathbf{E}}_o\cdot\mathbf{J}_V\cdot\dot{\mathbf{E}}_o$ reproduces the rigid inertial components of the angular momentum of the element.

The estimation of the potential energy can be carried out by extracting the contributions due to the deformation from the $\mathbf{u}_P$ motion. Then the projection of $\hat{\mathbf{u}}_P$ in (17) in the $\mathbf{E}_o^\xi$, $\mathbf{E}_o^\eta$, and $\mathbf{E}_o^\zeta$ directions gives the infinitesimal displacements:

$$\begin{aligned}\tilde{u} &= \hat{\mathbf{u}}_P \cdot \mathbf{E}_o^\xi = \varepsilon_o \xi - \tilde{\theta}^\zeta \eta - \tilde{\theta}^\eta \zeta,\\ \tilde{v} &= \hat{\mathbf{u}}_P \cdot \mathbf{E}_o^\eta = \varphi_o^\eta \xi - \tilde{\theta}^\xi \zeta,\\ \tilde{w} &= \hat{\mathbf{u}}_P \cdot \mathbf{E}_o^\zeta = \varphi_o^\zeta \xi + \tilde{\theta}^\xi \eta.\end{aligned} \tag{23}$$

By using this deformation kinematics, we define the following infinitesimal strain components of the $\boldsymbol{\varepsilon}_P$ tensor:

$$\begin{aligned}\varepsilon_{\xi\xi} &= \varepsilon_o - \tilde{\theta}^\zeta_{,\xi}\eta - \tilde{\theta}^\eta_{,\xi}\zeta,\\ \varepsilon_{\xi\eta} &= \frac{1}{2}\big(\varphi_o^\eta - \tilde{\theta}^\zeta - \omega^\zeta \tilde{\theta}^\xi_{,\xi}\big),\\ \varepsilon_{\xi\zeta} &= \frac{1}{2}\big(\varphi_o^\zeta - \tilde{\theta}^\eta + \omega^\eta \tilde{\theta}^\xi_{,\xi}\big),\end{aligned} \tag{24}$$

and $\varepsilon_{\eta\zeta} = 0$. In (24), shearing contributions due to the torsional mode are modeled by the $\omega^\eta(\eta,\zeta)$ and $\omega^\zeta(\eta,\zeta)$ functions. Here, because $h_\eta \times h_\zeta$ rectangular sections were analyzed, we assume the distributions:

$$\begin{aligned}\omega^\eta &= \frac{\eta^3}{(h_\eta/2)^2}\left(1 - \frac{\zeta^2}{(h_\zeta/2)^2}\right),\\ \omega^\zeta &= \frac{\zeta^3}{(h_\zeta/2)^2}\left(1 - \frac{\eta^2}{(h_\eta/2)^2}\right),\end{aligned} \tag{25}$$

where $\varepsilon_{\xi\eta} = 0$ and $\varepsilon_{\xi\zeta} = 0$ is realized on the boundaries $|\zeta| = h_\zeta/2$ and $|\eta| = h_\eta/2$ of the cross section, respectively.

Extensional components $\varepsilon_{\eta\eta}$ and $\varepsilon_{\zeta\zeta}$ are then obtained by imposing the statical assumptions $\sigma_{\eta\eta} = \sigma_{\zeta\zeta} = 0$ on the $\boldsymbol{\sigma}_P$ stress tensor. Then we have

$$\varepsilon_{\eta\eta} = \varepsilon_{\zeta\zeta} = -\frac{\lambda}{2(\lambda+\mu)}\varepsilon_{\xi\xi}, \tag{26}$$

where λ and μ are the Lamé coefficients. By using the (26) expressions, the remaining stress components are:

$$\begin{aligned}\sigma_{\xi\xi} &= 2\mu\varepsilon_{\xi\xi} + \lambda(\varepsilon_{\xi\xi} + \varepsilon_{\eta\eta} + \varepsilon_{\zeta\zeta}) = \frac{2\mu+3\lambda}{\lambda+\mu}\mu\varepsilon_{\xi\xi}\\ &= E\varepsilon_{\xi\xi},\\ \sigma_{\xi\eta} &= 2\mu\varepsilon_{\xi\eta} = 2G\varepsilon_{\xi\eta},\\ \sigma_{\xi\zeta} &= 2\mu\varepsilon_{\xi\zeta} = 2G\varepsilon_{\xi\zeta}\end{aligned} \tag{27}$$

and $\sigma_{\eta\zeta} = 0$. In (27), E and G are the Young and shear moduli, respectively.

By integrating over the section area the potential energy contribution, we have:

$$\begin{aligned}&\int_A \boldsymbol{\varepsilon}_P : \boldsymbol{\sigma}_P \, dA\\ &= \int_A \big(E\varepsilon_{\xi\xi}^2 + 4G\varepsilon_{\xi\eta}^2 + 4G\varepsilon_{\xi\zeta}^2\big)\, dA\\ &= E\Big(A\varepsilon_o^2 + J_\eta \tilde{\theta}^{\eta^2}_{,\xi} + J_\zeta \tilde{\theta}^{\zeta^2}_{,\xi}\Big)\\ &\quad + G\Big[A\big(\varphi_o^\eta - \tilde{\theta}_o^\zeta\big)^2\\ &\quad + \tilde{\theta}^{\xi^2}_{,\xi}\int_A \omega^{\xi^2} dA - 2\big(\varphi_o^\eta - \tilde{\theta}_o^\zeta\big)\tilde{\theta}^\xi_{,\xi}\int_A \omega^\zeta \, dA\Big]\\ &\quad + G\Big[A\big(\varphi_o^\zeta - \tilde{\theta}_o^\eta\big)^2\\ &\quad + \tilde{\theta}^{\xi^2}_{,\xi}\int_A \omega^{\eta^2} dA + 2\big(\varphi_o^\zeta - \tilde{\theta}_o^\eta\big)\tilde{\theta}^\xi_{,\xi}\int_A \omega^\eta \, dA\Big].\end{aligned} \tag{28}$$

Note that in (28), to overcome locking effects, the central value of the $\tilde{\theta}^\eta(\xi)$ and $\tilde{\theta}^\zeta(\xi)$ interpolations are used in the shear energy computation. Besides, assuming this, $\int_A \omega^\eta dA = \int_A \omega^\zeta \, dA = 0$ is obtained. Then, by defining $J_{\omega\eta} = \int_A \omega^{\eta^2} dA$ and $J_{\omega\zeta} = \int_A \omega^{\zeta^2} dA$, we can write:

$$\begin{aligned}\int_A \boldsymbol{\varepsilon}_P : \boldsymbol{\sigma}_P \, dA = E\Big(A\varepsilon_o^2 + J_\eta \tilde{\theta}^{\eta^2}_{,\xi} + J_\zeta \tilde{\theta}^{\zeta^2}_{,\xi}\Big)\\ + G\Big[A\big(\varphi_o^{\eta^2} + \varphi_o^{\zeta^2}\big)\\ + (J_{\omega\eta} + J_{\omega\zeta})\tilde{\theta}^{\xi^2}_{,\xi}\Big],\end{aligned} \tag{29}$$

with $\tilde{\theta}_o^\eta = \tilde{\theta}_o^\zeta = 0$. Then the potential energy is computed by further integration over the beam centerline:

$$\begin{aligned}U &= \frac{1}{2}\int_{-h_\xi/2}^{h_\xi/2}\int_A \boldsymbol{\varepsilon}_P : \boldsymbol{\sigma}_P \, dA \, d\xi\\ &= \frac{1}{2}E\Big[V\varepsilon_o^2 + \frac{1}{h_\xi}J_\eta\Big(D\tilde{\theta}^{\eta^2} + \frac{4}{3}S\tilde{\theta}^{\eta^2}\Big)\\ &\quad + \frac{1}{h_\xi}J_\zeta\Big(D\tilde{\theta}^{\zeta^2} + \frac{4}{3}S\tilde{\theta}^{\zeta^2}\Big)\Big]\\ &\quad + \frac{1}{2}G\Big[+V\big(\varphi_o^{\eta^2} + \varphi_o^{\zeta^2}\big)\\ &\quad + \frac{1}{h_\xi}(J_{\omega\eta} + J_{\omega\zeta})\Big(D\tilde{\theta}^{\xi^2} + \frac{4}{3}S\tilde{\theta}^{\xi^2}\Big)\Big].\end{aligned} \tag{30}$$

External work W, finally, is defined in (18) by the (16) and (17) expressions of the displacement vector. Note that kinematics of the element being modeled as a three-dimensional body, only external forces must be assigned. Besides, because finite rotations are replaced by products $\tilde{\theta}\mathbf{E}_o$ in the present formulation, we can

see from (17) that the external force vector is a linear function of the assumed unknowns.

5 Multibody systems

By referring to the previous beam element model, we can study the dynamical behavior of multibody systems. In particular, prismatic bodies linked by spherical joints and free mass particles are analyzed.

A prismatic $h_\xi \times h_\eta \times h_\zeta$ element is assumed such that only the ξ axial deformation ε is present. Springs in the joint point between elements produce, furthermore, restraint moments proportional to the relative rotations. In particular, we refer now to the $\mathbf{E}_n$ and $\mathbf{E}_m$ directors attached to the central points of the n and m elements and we denote with $D\theta^\xi$, $D\theta^\eta$ and $D\theta^\zeta$ the small relative rotations. We have:

$$\begin{aligned}
\mathbf{E}_m^\xi &= \mathbf{E}_n^\xi + D\theta^\eta \mathbf{E}_n^\eta + D\theta^\zeta \mathbf{E}_n^\zeta,\\
\mathbf{E}_m^\eta &= -D\theta^\eta \mathbf{E}_n^\xi + \mathbf{E}_n^\eta + D\theta^\xi \mathbf{E}_n^\zeta,\\
\mathbf{E}_m^\zeta &= -D\theta^\zeta \mathbf{E}_n^\xi - D\theta^\xi \mathbf{E}_n^\eta + \mathbf{E}_n^\zeta.
\end{aligned} \tag{31}$$

Then, by the usual manipulations, we obtain

$$\begin{aligned}
D\theta^\xi &= \frac{1}{2}\big(\mathbf{E}_n^\zeta \cdot \mathbf{E}_m^\eta - \mathbf{E}_n^\eta \cdot \mathbf{E}_m^\zeta\big),\\
D\theta^\eta &= \frac{1}{2}\big(\mathbf{E}_n^\eta \cdot \mathbf{E}_m^\xi - \mathbf{E}_n^\xi \cdot \mathbf{E}_m^\eta\big),\\
D\theta^\zeta &= \frac{1}{2}\big(\mathbf{E}_n^\zeta \cdot \mathbf{E}_m^\xi - \mathbf{E}_n^\xi \cdot \mathbf{E}_m^\zeta\big).
\end{aligned} \tag{32}$$

With the expression of the rigid component (16) and by zeroing the absent deformation measures in (17), the motion of the body is defined as

$$\begin{aligned}
\mathbf{u}_P = \mathbf{u} &+ \xi\big(\mathbf{E}^\xi - \mathbf{e}^\xi\big) + \eta\big(\mathbf{E}^\eta - \mathbf{e}^\eta\big)\\
&+ \zeta\big(\mathbf{E}^\zeta - \mathbf{e}^\zeta\big) + \xi\varepsilon\mathbf{E}^\xi,
\end{aligned} \tag{33}$$

where $\mathbf{u}$ is the central point displacement vector computed by the nodal values as in (14).

As before, the integration over the section area of the square of the velocity leads to

$$\begin{aligned}
&\int_A \dot{\mathbf{u}}_P \cdot \dot{\mathbf{u}}_P \, dA\\
&\quad = A\dot{\mathbf{u}} \cdot \dot{\mathbf{u}} + \xi^2 A\dot{\mathbf{E}}^\xi \cdot \dot{\mathbf{E}}^\xi + J_\zeta \dot{\mathbf{E}}^\eta \cdot \dot{\mathbf{E}}^\eta\\
&\qquad + J_\eta \dot{\mathbf{E}}^\zeta \cdot \dot{\mathbf{E}}^\zeta + 2\xi A\dot{\mathbf{u}} \cdot \dot{\mathbf{E}}^\xi\\
&\qquad + \xi^2 A\dot{\varepsilon}^2 + 2\xi A\dot{\varepsilon}\mathbf{E}^\xi \cdot \big(\dot{\mathbf{u}} + \xi\dot{\mathbf{E}}^\xi\big)
\end{aligned} \tag{34}$$

and, then to the kinetic energy evaluation by further integration on the ξ elemental domain

$$T = \frac{1}{2}\rho\big[V\dot{\mathbf{u}} \cdot \dot{\mathbf{u}} + \dot{\mathbf{E}} \cdot \mathbf{J}_V \cdot \dot{\mathbf{E}} + AJ_\xi\big(\dot{\varepsilon}^2 + 2\dot{\varepsilon}\mathbf{E}^\xi \cdot \dot{\mathbf{E}}^\xi\big)\big]. \tag{35}$$

In the potential energy definition. we refer to the EV axial rigidity and to the like type k_η, k_ζ flexural, and k_ξ torque stiffness:

$$U = \frac{1}{2}\big(EV\varepsilon^2 + k_\xi D\theta^{\xi^2} + k_\eta D\theta^{\eta^2} + k_\zeta D\theta^{\zeta^2}\big), \tag{36}$$

where the relative rotations are defined in (32) while axial deformation is defined in the first of (15) expressions:

$$g_I^\xi = \varepsilon - \frac{1}{h_\xi}\big[\mathbf{E}^\xi \cdot (\mathbf{u}_j - \mathbf{u}_i) - h_\xi + h_\xi E_x^\xi\big] = 0. \tag{37}$$

Finally, external energy W can be computed by the expression (33) of the displacement vector of the body.

We note that compatibility in the joint points between elements is realized because nodal displacements are assumed as unknowns of the element. However, internal rigidity of the body must be constrained by the $\varphi^\eta = 0$ and $\varphi^\zeta = 0$ conditions. Then, by the second and the third of (15) and the use of λ_I^η and λ_I^ζ Lagrange multipliers, in the energetic functional we add the contribution

$$\begin{aligned}
&\lambda_I^\eta g_I^\eta + \lambda_I^\zeta g_I^\zeta\\
&\quad = \lambda^\eta\big[\mathbf{E}^\eta \cdot (\mathbf{u}_j - \mathbf{u}_i) + h_\xi E_x^\eta\big]\\
&\qquad + \lambda^\zeta\big[\mathbf{E}^\zeta \cdot (\mathbf{u}_j - \mathbf{u}_i) + h_\xi E_x^\zeta\big].
\end{aligned} \tag{38}$$

In the three-dimensional mass particles motion, we refer to the ith particle of m_i mass. Potential energy of interaction of the particles i and j depends on the interbody distance $h_{ij} = (1 + \varepsilon_{ij})h$, where h is the initial distance and ε_{ij} is the related elongation. Then, by denoting with $\mathbf{u}_i$ the displacement vector of the particle and with k_a the interaction rigidity, kinetic, and potential energy are computed by referring to

$$T = \frac{1}{2}m_i\dot{\mathbf{u}}_i \cdot \dot{\mathbf{u}}_i, \qquad U = \frac{1}{2}k_a\varepsilon_{ij}^2. \tag{39}$$

For these models only, the use of the $\mathbf{E}^{ij}$ director in the direction from the ith to the jth particle is necessary. As usual, elongation is defined by

$$g_I^\xi = \varepsilon_{ij} - \frac{1}{h}\big[\mathbf{E}^{ij} \cdot (\mathbf{u}_j - \mathbf{u}_i) - h + hE_x^{ij}\big] = 0. \tag{40}$$

The internal connection between the $\mathbf{E}^{ij}$ director and the positions of the related particles is here imposed by the energetic contribution

$$\begin{aligned}
&\lambda_I^u g_I^u + \lambda_I^v g_I^v + \lambda_I^w g_I^w \\
&\quad = \lambda^u \big[u_j - u_i + h - E_x^{ij}(1+\varepsilon_{ij})h\big] \\
&\qquad + \lambda^v \big[v_j - v_i - E_y^{ij}(1+\varepsilon_{ij})h\big] \\
&\qquad + \lambda^w \big[w_j - w_i - E_z^{ij}(1+\varepsilon_{ij})h\big]. \qquad (41)
\end{aligned}$$

As we can see, constraints in (41) define the components of the $\mathbf{E}^{ij}$ vector in the inertial frame of reference.

6 Nonlinear dynamical analysis

We refer to dynamical systems with $L(\dot{\mathbf{q}}(t), \mathbf{q}(t))$ Lagrangian function obtained by summing the described energetic contributions, where $\mathbf{q}$ is the vector of the unknown components of the element. We denote with $\mathbf{g}_E = \mathbf{0}$ the constraint conditions in (3) relating the unknown components of the $\mathbf{E}^{\xi}$, $\mathbf{E}^{\eta}$, and $\mathbf{E}^{\zeta}$ vectors and with $\mathbf{g}_I = \mathbf{0}$ the internal compatibility conditions explicitly imposed in the description of the models. Related Lagrange multiplier vectors are denoted with $\boldsymbol{\lambda}_E$ and $\boldsymbol{\lambda}_I$, respectively.

Then we obtain the extended functional

$$\begin{aligned}
L^S(\mathbf{q}, \dot{\mathbf{q}}, \boldsymbol{\lambda}) &= T(\dot{\mathbf{q}}, \mathbf{q}) - U(\mathbf{q}) + W(\mathbf{q}) + \boldsymbol{\lambda}_E \cdot \mathbf{g}_E(\mathbf{q}) \\
&\quad + \boldsymbol{\lambda}_I \cdot \mathbf{g}_I(\mathbf{q}). \qquad (42)
\end{aligned}$$

In particular, for the beam element model we refer to the contributions given in (22) and (30) while $\mathbf{g}_I$ internal compatibility functions are established in (15). Unknown vector $\mathbf{q}$ is composed of the three u_i, v_i, w_i, displacements and the nine components of the directors $\mathbf{E}_i^{\xi}, \mathbf{E}_i^{\eta}, \mathbf{E}_i^{\zeta}$, at the nodes plus the nine components of the directors $\mathbf{E}_o^{\xi}, \mathbf{E}_o^{\eta}, \mathbf{E}_o^{\zeta}$, for each element. Six λ_E values for each $\mathbf{E}_i$ and $\mathbf{E}_o$ orthonormal system and three λ_I values for each elemental deformation complete the group of the unknowns. For the prismatic element model we use the expressions (35)–(38). The unknown vector is composed of the three u_i, v_i, w_i, nodal displacements and the nine components of the directors $\mathbf{E}^{\xi}, \mathbf{E}^{\eta}, \mathbf{E}^{\zeta}$, at the center of the element. As multipliers, then we have six λ_E and three λ_I unknown components. Mass particles motion, finally is described by the three u_i, v_i, w_i, displacements of the ith mass and the three E^{ij} components for each i–j connection. Energetic expressions are given in (39)–(41) where related multipliers are the three $\lambda_I^u, \lambda_I^v, \lambda_I^w$, components for the compatibility constraints and the λ_I^{ξ} component for the elongation measure definition.

By collecting $\boldsymbol{\lambda}_E$ and $\boldsymbol{\lambda}_I$ unknowns in the $\boldsymbol{\lambda}$ vector, the semidiscrete formulation of the motion can be written in the form:

$$\begin{aligned}
&\frac{\partial L}{\partial \mathbf{q}} - \frac{\partial}{\partial t}\frac{\partial L}{\partial \dot{\mathbf{q}}} = 0, \qquad \frac{\partial L}{\partial \boldsymbol{\lambda}} = 0, \\
&\mathbf{q}(0) = \mathbf{q}^*, \qquad \dot{\mathbf{q}}(0) = \dot{\mathbf{q}}^*, \qquad (43)
\end{aligned}$$

where $\mathbf{q}^*$ and $\dot{\mathbf{q}}^*$ represent the initial values and velocities, respectively.

For the time integration of the semidiscrete initial value problem (43) we refer to the constant time step $\Delta t = t_{n+1} - t_n$. Unknown components of the $\mathbf{q}$ and $\boldsymbol{\lambda}$ vectors also collected in the $\mathbf{d}$ vector. By assuming the state variables $\mathbf{d}_n$, $\dot{\mathbf{d}}_n$, $\ddot{\mathbf{d}}_n$, as known at the time t_n and making the external forces $\mathbf{p}(t)$ for all t, the time integration is restricted to the subsequent solution of the state variables at the end of each step $\mathbf{d}_{n+1}$, $\dot{\mathbf{d}}_{n+1}$, $\ddot{\mathbf{d}}_{n+1}$. In order to realize this step by step integration, the set of variables is reduced to the unknowns $\mathbf{d}_{n+1}$ only by the Newmark approximations

$$\begin{aligned}
\dot{\mathbf{d}}_{n+1} &= \frac{\gamma}{\beta \Delta t}(\mathbf{d}_{n+1} - \mathbf{d}_n) + \left(1 - \frac{\gamma}{\beta}\right)\dot{\mathbf{d}}_n \\
&\quad + \left(1 - \frac{\gamma}{2\beta}\right)\Delta t \ddot{\mathbf{d}}_n, \qquad (44) \\
\ddot{\mathbf{d}}_{n+1} &= \frac{1}{\beta \Delta t^2}(\mathbf{d}_{n+1} - \mathbf{d}_n) - \frac{1}{\beta \Delta t}\dot{\mathbf{d}}_n \\
&\quad + \left(1 - \frac{1}{2\beta}\right)\ddot{\mathbf{d}}_n. \qquad (45)
\end{aligned}$$

In the following, we use the average acceleration scheme by adopting $\gamma = 1/2$ and $\beta = 1/4$.

By inserting relations (44) and (45) in (43), we arrive at the nonlinear equation of the form:

$$\mathbf{F}(\mathbf{d}_{n+1}) = 0. \qquad (46)$$

This represents the nonlinear system of algebraic equations defined at the t_{n+1} time with the $\mathbf{d}_{n+1}$ unknown vector. The velocities and accelerations at the end of the time step can then be obtained by relations (44) and (45), respectively. Newton like iterative methods can be used to solve system (46) by linearization

$$\begin{aligned}
&\mathbf{F}\big(\mathbf{d}_{n+1}^{(k+1)}\big) \\
&\quad = \mathbf{F}\big(\mathbf{d}_{n+1}^{(k)}\big) + \frac{\partial \mathbf{F}(\mathbf{d}_{n+1}^{(k)})}{\partial \mathbf{d}_{n+1}}\big(\mathbf{d}_{n+1}^{(k+1)} - \mathbf{d}_{n+1}^{(k)}\big) \\
&\qquad + \mathbf{O}\big(\Delta t^2\big) = \mathbf{0}. \qquad (47)
\end{aligned}$$

The iterative process is here initialized by choosing $\mathbf{d}_{n+1}^{(0)}$ as the linear extrapolation of the previously computed $\mathbf{d}_n$ and $\mathbf{d}_{n-1}$ vectors when $n > 0$, while the formula $\mathbf{d}_1^{(0)} = \mathbf{d}^* + \Delta t \dot{\mathbf{d}}^*$ is used when $n = 0$. By choosing the fixed tolerance $\eta = 10^{-8}$, the formula

$$\left\|\mathbf{d}_{n+1}^{(k+1)} - \mathbf{d}_{n+1}^{(k)}\right\| / \left\|\mathbf{d}_{n+1}^{(k+1)} - \mathbf{d}_n\right\| \leq \eta \tag{48}$$

is adopted as convergence criterion.

We note that the use of the $\mathbf{g}_E = \mathbf{0}$ constraint equations are necessary for the description of the element model. The use of the $\mathbf{g}_I = \mathbf{0}$ explicit internal constraint equations instead can be avoided by the intrinsic definition of the related parameters with resulting decrease in the number of unknowns. Such a benefit, nevertheless, is balanced by an increase in the complexity in the evaluation of the coefficients in the algebraic system and a larger band in the iteration matrix. Similar computational characteristics in terms of computation time and approximation, however, can be verified in both cases.

Here, the use of the constraint equations is suitable for improving stability in the time integration scheme. As shown in [11], the use of a time relaxed description of the connection between deformation and rotational parameters leads to an appreciable increase in the range of stability of the time integration scheme and a reduction in the number of Newton iterations required in the time integration step. Such a relaxed description is obtained by referring to the extended functional

$$\begin{aligned} L^R(\mathbf{q}, \dot{\mathbf{q}}, \boldsymbol{\lambda}) &= T(\dot{\mathbf{q}}, \mathbf{q}) - U(\mathbf{q}) + W(\mathbf{q}) + \boldsymbol{\lambda}_E \cdot \dot{\mathbf{g}}_E(\mathbf{q}) \\ &\quad + \boldsymbol{\lambda}_I \cdot \dot{\mathbf{g}}_I(\mathbf{q}), \end{aligned} \tag{49}$$

where the constraint equations are replaced by their time differentiations. In such a representation, we note that consistent initial conditions for directors and deformations must be provided to preserve $\mathbf{g}_E(\mathbf{q}) = 0$ and $\mathbf{g}_I(\mathbf{q}) = 0$.

In the following, we denote the (42) and (49) functionals as the strong and relaxed form of the Lagrangian formulation respectively. Similarly, related nonlinear Newmark integration algorithms are denoted by L^S and L^R schemes, respectively.

7 Numerical tests

A set of numerical examples shows the application of the proposed method for the time integration of the motion equations. Stable behavior of the time integration method, in the absence of numerical dissipation, is verified by referring to the condition

$$\Delta E = U_{n+1} - U_n + T_{n+1} - T_n - \Delta W = 0, \tag{50}$$

as a sufficient stability condition in the nonlinear dynamical schemes (see, e.g., [1], [3]). Equation (50) expresses the conservation of the total energy ΔE, where U_{n+1} and U_n represent the internal energy at the end and the beginning of the time step, T_{n+1} and T_n being the corresponding kinetic energy and ΔW symbolizing the work done by external forces within the time step. We use the trapezoidal rule to calculate the work of the external forces:

$$\Delta W = \frac{1}{2}(\mathbf{u}_{n+1} - \mathbf{u}_n) \cdot (\mathbf{p}_{n+1} + \mathbf{p}_n). \tag{51}$$

As regards consistency note that as in the numerical tests, for such a Δt in which both L^S and L^R representations have a stable behavior, the difference between respective kinematic quantities of interest proves to be negligible. In this way, the methods prove to be second-order accurate.

Numerical tests were performed for increasing values of the Δt time step. Let *steps* be the number of time steps effected by the integration process to analyze the behavior for $t = 0 \ldots T$. In the following, we refer to the mean value of the Nw_i Newton iterations in the ith step

$$Nw_m = \sum_{i=1}^{step} Nw_i / steps, \tag{52}$$

carried out, unless it becomes unstable (*div*), in the process.

7.1 Motion of a dumbbell

We investigate the motion of a dumbbell with initial interbody distance $h = 1$ modeled as a two-particle problem and defined in the three-dimensional ambient space. We assume $m_1 = m_2 = 1$ with $\mathbf{u} = \{u_1\ v_1\ w_1\ u_2\ v_2\ w_2\}$. The initial conditions are given by $\mathbf{u}^* = \mathbf{0}$, $\dot{\mathbf{u}}^* = \{0\ 0\ 2\ 5\ 5\ 10\}$ and $\mathbf{E}^{ij} = \{1\ 0\ 0\}$ is the director in the x direction. Accordingly, $\varepsilon_{ij} = 0$ and, by time differentiation of expressions (40) and (41), $\dot{\varepsilon}_{ij} = 0$ and $\dot{\mathbf{E}}^{ij} = \{0\ 3\ 5\}$ is obtained.

The interaction of the two bodies is assumed to be governed by a Lennard–Jones potential $U(r_{ij}) = A[(\sigma/r_{ij})^5 - (\sigma/r_{ij})^3]$ which is often employed in

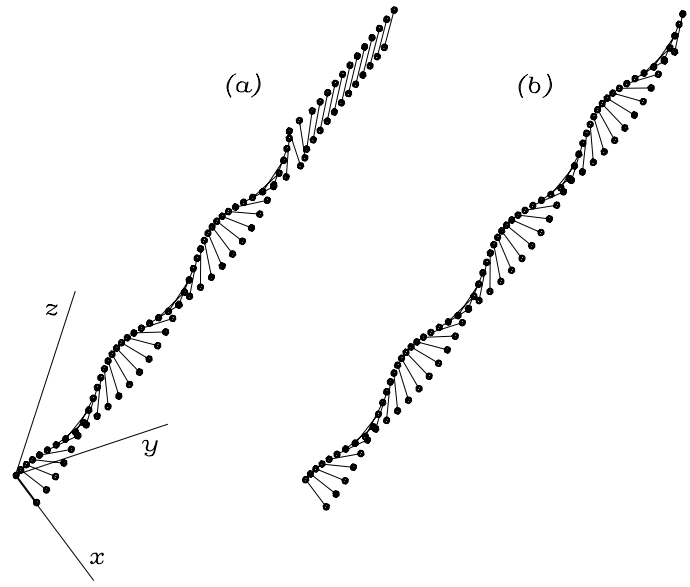

Fig. 2 Dumbbell $\Delta t = 0.02$ for $T = 2$: sequence of configurations obtained by the (**a**) L^S and (**b**) L^R scheme, respectively

molecular dynamic simulations. The distance between the centers of the two particles is $r_{ij} = h + \varepsilon_{ij}$. We make $\sigma = (3/5)^{1/2}$, such that $\varepsilon_{ij} = 0$ characterizes the internal force free configuration. Here, we consider the quasi-rigid connection $A = 10^6$ that classically has severe instability restrictions. In such a case, by linearization of $U(r_{ij})$ for $r_{ij} = 1$, $k_a = 6A\sigma^3$ can be interpreted as the spring stiffness. We can refer to Gonzales and Simo [27] and Crisfield and Shi [28] for the numerical instabilities which are introduced in such dynamic systems. Additional background material on the motion of a several particle system in a potential field can be found in standard books on classical mechanics; see, e.g., Goldstein [25] and Arnold [26].

To illustrate the motion, Fig. 2 contains a sequence of configurations calculated in the L^S and L^R representation with $\Delta t = 0.02$ and $t = 0 \ldots 2$. At about $t = 1.4$ an unphysical motion indicates the unstable behavior of the Newmark scheme in the L^S representation. Related evolutions of the (50) increment of total energy are plotted in Fig. 3. The incipient non stable behavior is highlighted because the total energy oscillates and increases up until unbounded values. L^R representation always shows oscillations contained in the neighborhood of zero. As $\mathbf{p} = \mathbf{0}$ is problem with nonzero initial values, in (50) the value of ΔW is replaced by the initial kinetic energy. Table 1 finally reports the mean value (52) of Newton iterations carried out in the process for $T = 10$ in both schemes.

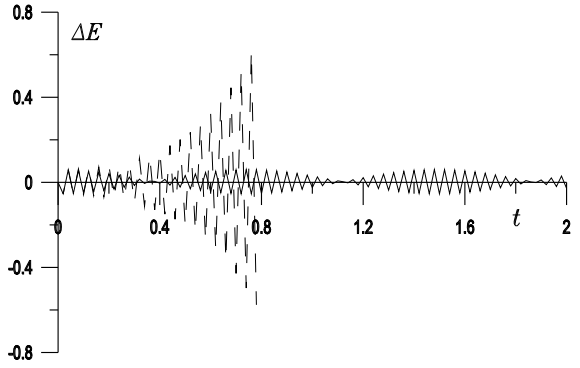

Fig. 3 Dumbbell $\Delta t = 0.02$ for $T = 2$: total energy increment ΔE versus time t; *dotted line* for L^S and continuous line for L^R representations, respectively

7.2 Two body system

Here, we study the behavior of a pair of equal pin-jointed elements as described in Sect. 5. Starting from rest, the dynamics of the two prismatic $h_\xi = 0.5$, $h_\eta = h_\zeta = 0.02$, bodies is stimulated by an impulsive force $p(t)$ acting on the system as illustrated in Fig. 4. We assume $\rho = 1.5 \times 10^4$ and $E = 5 \times 10^9$, $k_\xi = 10^3$, $k_\eta = 5 \times 10^2$, $k_\zeta = 2 \times 10^2$, for the evaluation of the (35) kinetic and (36) potential energy. Time-stepping schemes applied to N-body problems can be found in Betsch and Steinmann [10].

The motion of the two body system, computed in both representations with $\Delta t = 0.0002$ and $T = 0.3$,

Table 1 Dumbbell $T = 10$: mean value Nw_m of the Newton iterations

Δt	0.002	0.005	0.01	0.02	0.05	0.1
L^S-scheme	3.000	3.185	3.486	*div*		
L^R-scheme	2.665	2.986	3.050	3.575	4.100	5.000

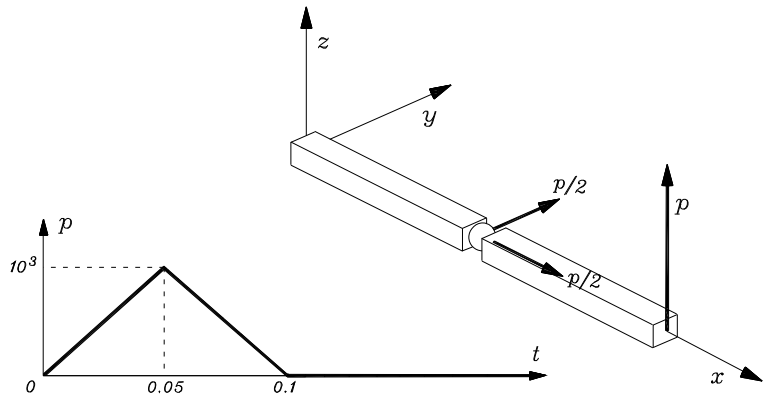

Fig. 4 Two body system: initial configuration and problem definition

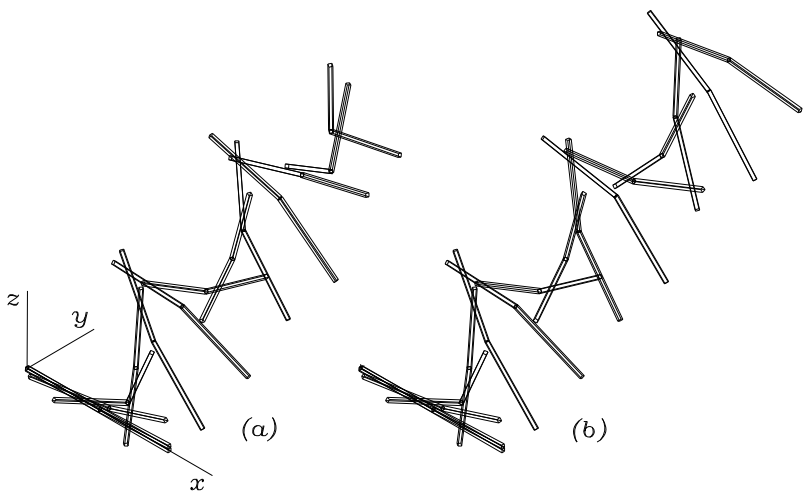

Fig. 5 Two body system $\Delta t = 0.0002$ for $T = 0.3$: sequence of configurations obtained by the (**a**) L^S and (**b**) L^R scheme, respectively

is shown in Fig. 5. The unstable motion of the system in the L^S representation can be observed at about $t = 0.21$ where chaotic relative rotations in the joint point occur. The reason for this behavior can be identified by means of the time histories of energy given in Fig. 6. A stable and conservative behavior of the L^R scheme can be verified by the time histories reported in Fig. 7. Applications of L^S and L^R representations for increasing values of the time step Δt are then investigated. Table 2 reports the Nw_m values performed in the time integration process for $T = 1$.

7.3 Toss rule in space

The characteristics of the time-integration scheme applied to the different Lagrangian representations will be shown here for the example of the three-dimensional movement of a toss rule (see Kuhl and Ramm [29] for a solution to such a dynamical problem). The beam, with zero initial displacements and velocities, is discretized by nine described finite elements. The geometry, position of loads, and load function of the rule are described in Fig. 8. The material is characterized by the values $\rho = 7.8 \times 10^3$, $E = 2.06 \times 10^{11}$ and $G = E/2$.

Table 2 Two body system $T = 1$: mean value Nw_m of the Newton iterations

Δt	0.00002	0.00005	0.0001	0.0002	0.0005	0.001	0.002
L^S-scheme	3.010	3.312	3.665	*div*			
L^R-scheme	2.045	2.518	2.965	3.004	3.777	3.965	4.892

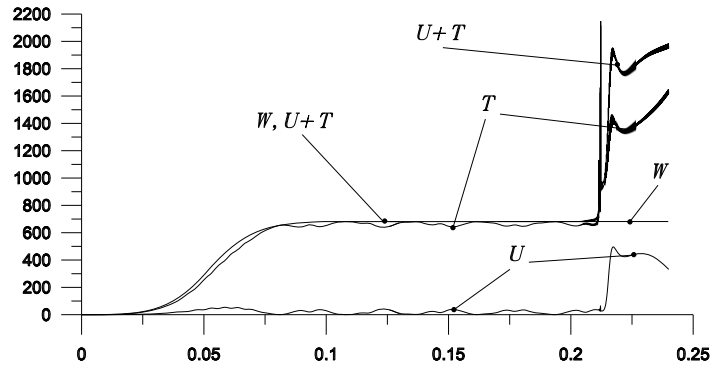

Fig. 6 Two body system $\Delta t = 0.0002$ for $T = 0.3$: energy versus time for L^S representation

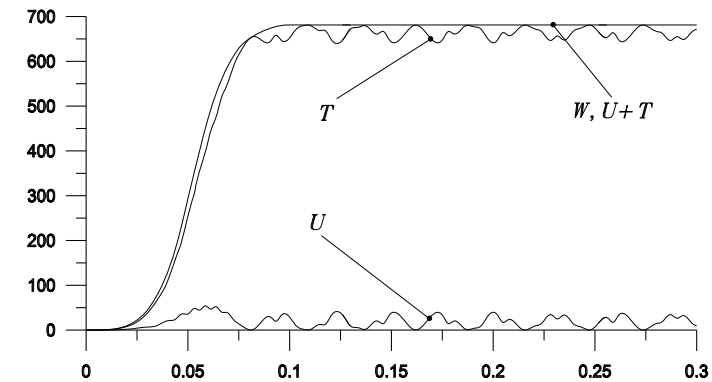

Fig. 7 Two body system $\Delta t = 0.0002$ for $T = 0.3$: energy versus time for L^R representation

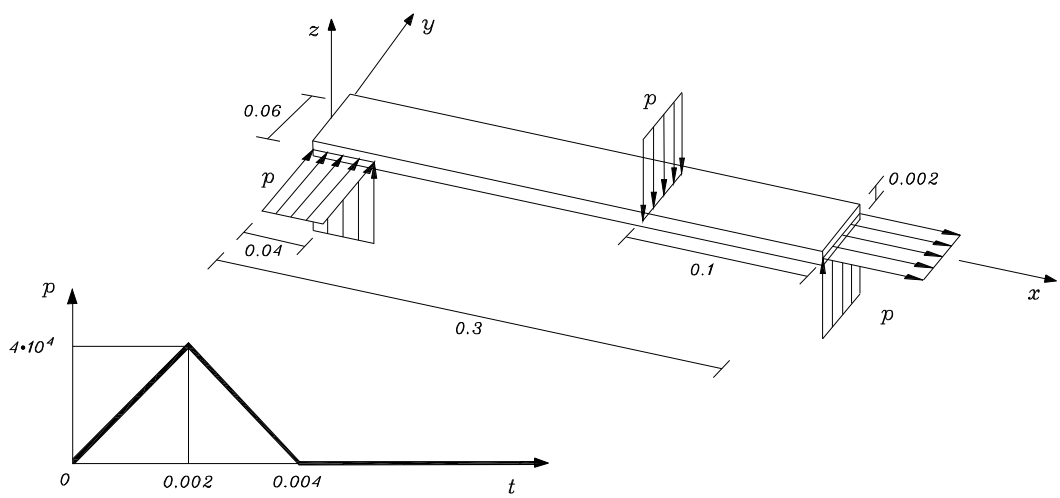

Fig. 8 Toss rule: geometry, loads and load function

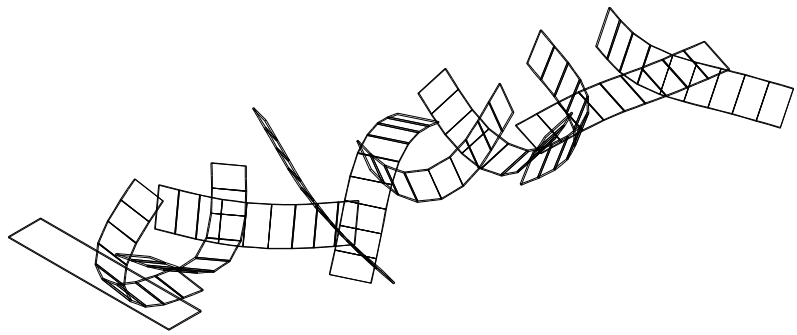

Fig. 9 Toss rule $\Delta t = 0.00005$ for $T = 0.04$: sequence of configurations obtained by the L^R scheme

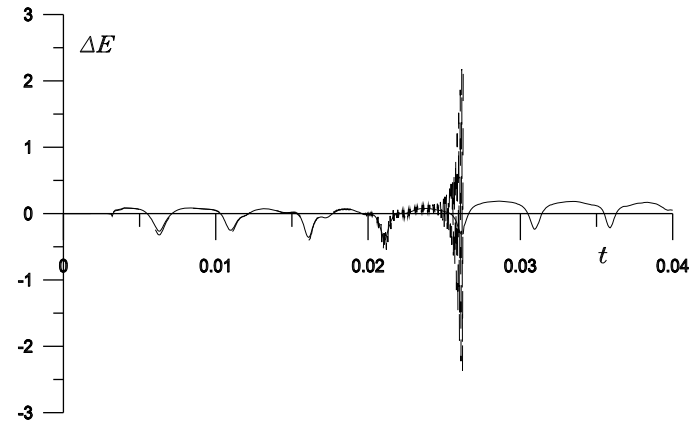

Fig. 10 Toss rule $\Delta t = 0.00005$ for $T = 0.04$: total energy increment ΔE versus time t; dotted line for L^S and continuous line for L^R representations, respectively

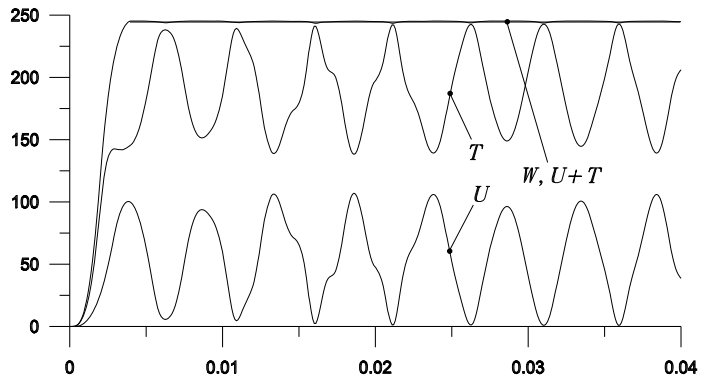

Fig. 11 Toss rule $\Delta t = 0.0001$ for $T = 0.04$: energy versus time for L^R representation

Selected deformed configurations computed within the $t = 0 \ldots 0.04$ time by the L^R representation are shown in Fig. 9. A stable behavior of the L^R scheme is obtained. Figure 10 shows total energy increment versus time with $\Delta t = 0.00005$ for both representations. An incipient nonstable behavior of the integration scheme in the L^S representation at about $t = 0.026$ can be observed, while bounded oscillations in the neighborhood of zero value can be verified in the L^R representation.

For the L^R scheme with $\Delta t = 0.0001$, the time histories of energy are given in Fig. 11. Finally, Table 3 shows the behavior of the two different schemes with respect to the time integration step for $T = 0.1$. We note that, although a long time stable behavior is observed also for large Δt, weak disagreements between the W and $U + T$ values are recorded.

Table 3 Toss rule $T = 0.1$: mean value Nw_m of the Newton iterations

Δt	0.00001	0.00002	0.00005	0.0001	0.0002	0.0005
L^S-scheme	3.202	3.635	*div*			
L^R-scheme	2.104	2.478	3.000	3.225	4.360	4.970

8 Conclusions

In the hypothesis of large rotations and small strains, a technique to analyze the dynamical behavior of three-dimensional finite element beam frames has been presented. A vectorial approach for the rotation parameterizations and linear strain definitions based on slope unknowns has been used. The analyzed models do not use angle measures and a total Lagrangian and implicitly conservative mechanical description of the motion is obtained.

The use of relaxed representations in the internal strains—rotations compatibility appears to significantly improve the behavior of the time integration scheme with regard to stability. In the numerical applications of the approach, it can be seen that the variation in the total energy in the time steps has bounded oscillations about the zero value. Arbitrary implicit one-step time integration schemes with Newmark approximations are suitable for use as basic algorithms for the proposed procedure. Finite element assembling procedures, moreover, are unchanged by maintaining their typical local nature.

The tests show a good convergence of the internal Newton iteration. The increase in computational effort due to the introduction of new unknowns and the loss of symmetry in the iteration matrix is balanced by this reduction in the number of Newton iterations required in the time integration steps. The computed equilibrium paths are in agreement with the results reported in the literature for similar models and the stability in the solution process has been shown to be insensitive to large incremental steps, at least for acceptable time increments in regard to the approximation error.

References

1. Belytschko, T., Schoeberle, D.F.: On the unconditional stability of an implicit algorithm for nonlinear structural dynamics. J. Appl. Mech. **42**, 865–869 (1975)
2. Hughes, T.J.R., Caughy, T.K., Liu, W.K.: Finite-element methods for nonlinear elastodynamics which conserve energy. J. Appl. Mech. **45**, 366–370 (1978)
3. Simo, J.C., Tarnow, N.: The discrete energy-momentum method. Conserving algorithms for nonlinear elastodynamics. J. Appl. Math. Phys. **43**, 757–792 (1992)
4. Simo, J.C., Tarnow, N.: A new energy and momentum conserving algorithm for the nonlinear dynamics of shells. Int. J. Numer. Methods Eng. **37**, 2527–2549 (1994)
5. Kuhl, D., Ramm, E.: Generalized energy-momentum method for non-linear adaptive shell dynamics. Comput. Methods Appl. Mech. Eng. **178**, 343–366 (1999)
6. Hoff, C., Pahl, P.J.: Development of an implicit method with numerical dissipation for generalized single step algorithm for structural dynamics. Comput. Methods Appl. Mech. Eng. **67**, 367–385 (1988)
7. Chung, J., Hulbert, G.M.: A time integration algorithm for structural dynamics with improved numerical dissipation: the generalized-a method. J. Appl. Mech. **60**, 371–375 (1993)
8. Zienkiewicz, O.C., Wood, W.L., Hine, N.W., Taylor, R.L.: A unified set of single step algorithms. Part I: general formulation and applications. Int. J. Numer. Methods Eng. **20**, 1529–1552 (1984)
9. Lasaint, P., Raviart, P.A.: On a finite element method for solving the neutron transport equation. In: de Boor C. (ed.) Mathematical Aspects of Finite Elements in Partial Differential Equations, pp. 89–123. Academic Press, New York (1974)
10. Betsch, P., Steinmann, P.: Conservation properties of a time FE method. Part I: time-stepping schemes for N-body problems. Int. J. Numer. Methods Eng. **49**, 599–638 (2000)
11. Lopez, S.: Changing the representation and improving stability in time-stepping analysis of structural non-linear dynamics. Nonlinear Dyn. **46**, 337–348 (2006)
12. Gear, C.W., Petzold, L.R.: ODE methods for the solution of differential/algebraic systems. SIAM J. Numer. Anal. **21**, 716–728 (1984)
13. Bachmann, R., Brüll, L., Mrziglod, T., Pallaske, U.: On methods for reducing the index of differential algebraic equations. Comput. Chem. Eng. **14**, 1271–1273 (1990)
14. Mattsson, S.E., Söderlind, G.: Index reduction in differential-algebraic equations using dummy derivatives. SIAM J. Sci. Comput. **14**, 677–692 (1993)
15. Belytschko, T., Hsieh, B.J.: Non-linear transient finite element analysis with convected co-ordinates. Int. J. Numer. Methods Eng. **7**, 255–271 (1973)
16. Argyris, J.: An excursion into large rotations. Comput. Methods Appl. Mech. Eng. **32**, 85–155 (1982)
17. Rankin, C.C., Nour-Omid, B.: The use of projectors to improve finite element performance. Comput. Struct. **30**, 257–267 (1988)
18. Cardona, A., Geradin, M.: A beam finite element non-linear theory with finite rotations. Int. J. Numer. Methods Eng. **26**, 2403–2438 (1988)

19. Crisfield, M.A.: A consistent co-rotational formulation for nonlinear three-dimensional beam elements. Comput. Methods Appl. Mech. Eng. **81**, 131–150 (1990)
20. Ibrahimbegović, A., Shakourzadeh, H., Batoz, J.L., Al Mikdad, M., Guo, Y.Q.: On the role of geometrically exact and second-order theories in buckling and post-buckling analysis of three-dimensional beam structures. Comput. Struct. **61**, 1101–1114 (1996)
21. Lopez, S., La Sala, G.: A vectorial approach for the formulation of finite element beams in finite rotations. In: Proceedings Tenth International Conference on Computational Structures Technology. Valencia (2010)
22. Lopez, S.: A three-dimensional beam element undergoing finite rotations based on slopes and distance measures. Internal Report, Dipartimento di Modellistica per l'Ingegneria, Università della Calabria, p. 53 (2010)
23. Betsch, P., Steinmann, P.: Constrained integration of rigid body dynamics. Comput. Methods Appl. Mech. Eng. **191**, 467–488 (2001)
24. Betsch, P., Steinmann, P.: Constrained dynamics of geometrically exact beams. Comput. Mech. **31**, 49–59 (2003)
25. Goldstein, H.: Classical Mechanics. Addison-Wesley, Reading (1980)
26. Arnold, V.I.: Mathematical Methods of Classical Mechanics. Prentice-Hall, Englewood Cliffs (1989)
27. Gonzales, O., Simo, J.C.: On the stability of symplectic and energy-momentum algorithms for non-linear Hamiltonian systems with symmetry. Comput. Methods Appl. Mech. Eng. **134**, 197–222 (1996)
28. Crisfield, M.A., Shi, J.: An energy conserving co-rotational procedure for non-linear dynamics with finite elements. Nonlinear Dyn. **9**, 37–52 (1996)
29. Kuhl, D., Ramm, E.: Constraint energy momentum algorithm and its application to non-linear dynamics of shells. Comput. Methods Appl. Mech. Eng. **136**, 293–315 (1996)